Control of rotation-floating space robots with flexible appendages for on-orbit servicing

Sofiane Kraiem, Mathieu Rognant, Jean-Marc Biannic, Yves Briere

Control of rotation-floating space robots with flexible appendages for on-orbit servicing

Sofiane Kraïem[1] and Mathieu Rognant[2] and Jean-Marc Biannic[3] and Yves Brière[4]

Abstract— **On-orbit operations are facing a growing need for autonomous robotic systems. Debris removal, on-orbit servicing and in-space deployment/assembly are examples of applications considering the use of robot manipulators. This paper addresses design and control problems related to autonomous space manipulator systems when using kinetic moment exchange devices in presence of flexible appendages. The paper introduces a method to develop a common control of the spacecraft base and manipulator. An extended state observer is used in the Nonlinear Dynamic Inversion (NDI) in order to improve performances and reduce vibration disturbance impacts on the base attitude. A simultaneous synthesis of a control law and an observer gain is proposed with Linear Matrix Inequalities (LMI) resolutions which allow system variation considerations. Simulations are run on an actual assembly scenario to illustrate the proposed method.**

I. Introduction

Robotic systems are predicted to play a key role in near-future space missions as unmanned missions and large structures that cannot be self-deployed as a single piece will become more common [1]. Yet, for in-space capture, deployment and on-orbit servicing operations, robotic systems will require to become autonomous to be a viable solution [2]. The recent evolution on space telescope programs allows to illustrate that need of new technologies for in-space deployment. Recent studies consider the use of autonomous manipulators to allow the self-deployment of telescope's mirror [3]. Future on-orbit deployed satellites will commonly have to be equipped with light and large appendages such as solar arrays, antennas and solar shields. Furthermore, the size and weight of each element will lead to some flexibility to be considered to fulfill the space mission objectives.

The appendages vibrations not only affect the base attitude and drift but also the manipulator motions. Active control has been proposed to cancel vibrations, using piezoelectric actuators placed on the flexible appendage [4] or with joint variable stiffness control actuators [5]. Yet, active control shows limitations for large on-orbit structures with limited actuators in order to compensate the vibrations in an energy efficient way. In terms of passive control, as it may be difficult to obtain the flexible dynamics, controller robust to unknown disturbances have been proposed [6].

Achieving attitude control during the manipulator maneuvers remain a challenging task as in addition to external torques/forces, manipulator motions and appendages vibrations may create undesired base rotations. Efficient use of thrusters to compensate manipulator motions have been studied through workspace adjustment strategies [7], or simultaneous control of the global center of mass and spacecraft attitude [8]. Likewise, when only the manipulator is controlled reaction null-space control has been developed to reduce interactions between the manipulator and the spacecraft base [9]. In presence of flexible appendages, as vibrations are partly due to manipulator motions, based on coupling factors between the manipulator rigid dynamics and the appendages flexible dynamics a control strategy has been proposed to suppress the vibrations [10] or an optimization of manipulator trajectories to minimize base disturbances has also been suggested [11].

Moreover, future missions are expected to have longer lifespan. Besides efficient propellant consumption strategies of the flying space manipulators, a meaningful way to increase the lifespan is the use of kinetic moment exchange devices with electrical which are addressed as rotation free-floating spacecraft-manipulator [12]. Controlling the manipulator capitalizing on the benefits of kinetic moment exchange devices has raised an interest to deal with the manipulation of relatively high mass and inertia such as in capture or deployment scenarios. Through kinematic indices, controlling the spacecraft attitude while controlling the manipulator allows to increase its manipulability [13]. Combining reaction wheels and control moment gyroscopes has been studied to maintain the satellite platform fixed during manipulator motions [14].

This paper aims at developing the common control of the spacecraft base and manipulator under structural disturbances for on-orbit deployment applications. An interest to develop a common control is highlighted when considering the system momentum distribution for different manipulator configurations [13]. This paper contribution resides in the integration of the flexible dynamics to the rigid dynamics, allowing to develop an extended state observer to improve the control performances, instead of an unknown disturbance observer for a rigid system [6]. The system is then decoupled and linearized with an NDI including the estimation of the vibration disturbances and the spacecraft drift. Moreover the synthesis of the control law and observer is developed for realistic large dimension systems.

[1] Sofiane Kraïem is with L'Institut supérieur de l'aéronautique et de l'espace, 10 Avenue Edouard Belin, 31055 Toulouse, France sofiane.kraiem@isae-supaero.fr

[2]Mathieu Rognant is with ONERA, 2 Avenue Edouard Belin, 31000 Toulouse, France mathieu.rognant@onera.fr

[3]Jean-Marc Biannic is with ONERA, 2 Avenue Edouard Belin, 31000 Toulouse, France jean-marc.biannic@onera.fr

[4] Yves Brière is with L'Institut supérieur de l'aéronautique et de l'espace, 10 Avenue Edouard Belin, 31055 Toulouse, France o.fr

This paper is organised as follows, firstly the dynamics of a rotation free-floating spacecraft with a rigid manipulator and flexible appendages are detailed, secondly a common control of the manipulator and the spacecraft base attitude is developed and thirdly the proposed method efficiency is illustrated on an on-orbit telescope deployment.

II. System open-loop dynamics

A. Problem statement

In this paper, a free-floating spacecraft actuated with n_r reaction wheels is considered. one serial-link manipulator with n_q degrees of freedom (DOF) is mounted on the satellite base The manipulator joints are either prismatic or revolute joints. Moreover, flexible appendages, such as solar arrays or solar shields, are connected to the base spacecraft. In this paper, the vibrations and the base linear dynamics are not measured, only manipulator joint velocity and pose and base attitude dynamics are available. In this study, neither environmental nor external forces are considered here and no initial momentum hypothesis are made.

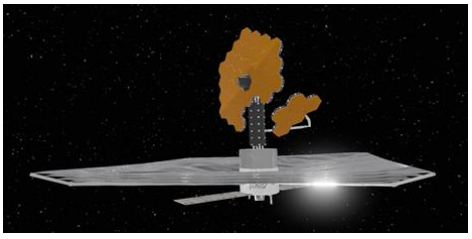

Fig. 1: Illustration of the studied spacecraft [3]

B. Dynamics of a rigid space manipulator with flexible appendages

The dynamics of a rigid multi-body system with no external forces applied to it, can be expressed as in [13]:

$$\underbrace{\begin{bmatrix}\mathbf{H}_0 & \mathbf{H}_{0q}\\ \mathbf{H}_{0q}^T & \mathbf{H}_q\end{bmatrix}}_{\mathbf{H}(\mathbf{q})}\begin{bmatrix}\dot{\mathbf{u}}_0\\ \ddot{\mathbf{q}}\end{bmatrix}+\underbrace{\begin{bmatrix}\mathbf{C}_0 & \mathbf{C}_{0q}\\ \mathbf{C}_{0q}^T & \mathbf{C}_q\end{bmatrix}}_{\mathbf{C}(\mathbf{q},\dot{\mathbf{q}},\mathbf{u}_0)}\begin{bmatrix}\mathbf{u}_0\\ \dot{\mathbf{q}}\end{bmatrix}=\begin{bmatrix}\mathbf{0}\\ \boldsymbol{\tau}_q\end{bmatrix} \quad (1)$$

where $\mathbf{u}_0 = \begin{bmatrix}\boldsymbol{\omega}_0^T & \dot{\mathbf{p}}_0^T\end{bmatrix}^T \in \mathbb{R}^{6\times 1}$ is the base spacecraft angular and linear velocity vector, $\dot{\mathbf{q}} = \begin{bmatrix}\dot{\mathbf{q}}_r^T & \dot{\mathbf{q}}_m^T\end{bmatrix}^T \in \mathbb{R}^{n_q\times 1}$ (with $n_q = n_r + n_m$) is the reaction wheels and joint velocity vector and $\boldsymbol{\tau}_q = \begin{bmatrix}\boldsymbol{\tau}_r^T & \boldsymbol{\tau}_m^T\end{bmatrix}^T \in \mathbb{R}^{n_q\times 1}$ the actuator torques.

$\mathbf{H}$ is a nonlinear matrix, symmetric and positive-definite corresponding to the generalized inertia matrix including both the inertia coupling matrices between the base and the manipulator, $\mathbf{H}_{0m}$, and between the base and the kinetic moment exchange devices, $\mathbf{H}_{0r}$. $\mathbf{C}$ is the convective inertia matrix which is a nonlinear matrix.

In order to incorporate the flexible dynamics of an appendage connected to the spacecraft base at point P, one can use the generic second order equation of the hybrid-cantilvered model [15].

$$\begin{bmatrix}\mathbf{H}_0^P & \mathbf{L}_P^T\\ \mathbf{L}_P & \mathbf{I}_{n_\eta}\end{bmatrix}\begin{bmatrix}\mathbf{a}_p\\ \ddot{\boldsymbol{\eta}}\end{bmatrix}+\begin{bmatrix}\mathbf{0}_{n_\eta} & \mathbf{0}_{n_\eta}\\ \mathrm{diag}(2\zeta_i\omega_i) & \mathrm{diag}(\omega_i^2)\end{bmatrix}\begin{bmatrix}\dot{\boldsymbol{\eta}}\\ \boldsymbol{\eta}\end{bmatrix}=\begin{bmatrix}\boldsymbol{\tau}_{ext}^P\\ \mathbf{0}\end{bmatrix} \quad (2)$$

where η is the modal coordinate vector of the n_η flexible modes, ω_i and ζ_i are respectively the angular frequency and damping ratios of the i^{th} mode, $\mathbf{L}_P$ is the vector of the modal participation at the connection point P, $\mathbf{H}_0^P$ is the spacecraft base generalized inertial matrix expressed at the point P, and $\mathbf{a}_p$ and $\boldsymbol{\tau}_{ext}^P$ are respectively the spacecraft acceleration screw and the external forces expressed at the point P.

Combining (1) and (2) with the assumption of no external forces/torques applied either on the system and on the links between the flexible appendages and the spacecraft we obtain the full dynamics of a rigid-flexible multi-body:

$$\begin{bmatrix}\mathbf{H}_\omega & \mathbf{H}_{\omega L} & \mathbf{H}_{\omega q} & \mathbf{H}_{\omega\eta}\\ \mathbf{H}_{L\omega} & \mathbf{H}_L & \mathbf{H}_{Lq} & \mathbf{H}_{L\eta}\\ \mathbf{H}_{\omega q}^T & \mathbf{H}_{Lq}^T & \mathbf{H}_q & \mathbf{0}\\ \mathbf{H}_{\omega\eta}^T & \mathbf{H}_{L\eta}^T & \mathbf{0} & \mathbf{H}_\eta\end{bmatrix}\begin{bmatrix}\dot{\boldsymbol{\omega}}_0\\ \ddot{\mathbf{p}}_0\\ \ddot{\mathbf{q}}\\ \ddot{\boldsymbol{\eta}}\end{bmatrix}+\begin{bmatrix}\mathbf{C}_\omega & \mathbf{C}_{\omega L} & \mathbf{C}_{\omega q} & \mathbf{C}_{\omega\eta}\\ \mathbf{C}_{L\omega} & \mathbf{C}_L & \mathbf{C}_{Lq} & \mathbf{C}_{L\eta}\\ \mathbf{C}_{\omega q}^T & \mathbf{C}_{Lq}^T & \mathbf{C}_q & \mathbf{0}\\ \mathbf{C}_{\omega\eta}^T & \mathbf{C}_{L\eta}^T & \mathbf{0} & \mathbf{C}_\eta\end{bmatrix}\begin{bmatrix}\boldsymbol{\omega}_0\\ \dot{\mathbf{p}}_0\\ \dot{\mathbf{q}}\\ \dot{\boldsymbol{\eta}}\end{bmatrix}+\begin{bmatrix}\mathbf{0} & \mathbf{0} & \mathbf{0} & \mathbf{0}\\ \mathbf{0} & \mathbf{0} & \mathbf{0} & \mathbf{0}\\ \mathbf{0} & \mathbf{0} & \mathbf{0} & \mathbf{0}\\ \mathbf{0} & \mathbf{0} & \mathbf{0} & \mathbf{K}_\eta\end{bmatrix}\begin{bmatrix}\boldsymbol{\theta}_0\\ \mathbf{p}_0\\ \mathbf{q}\\ \boldsymbol{\eta}\end{bmatrix}=\begin{bmatrix}\mathbf{0}\\ \mathbf{0}\\ \boldsymbol{\tau}_q\\ \mathbf{0}\end{bmatrix} \quad (3)$$

We decompose the base angular and linear contribution on the base in (3), using subscripts $_L$ and $_\omega$ respectively to indicate the linear and angular contribution of each matrix.

C. Simulation tools

In order to proceed to numerical simulations, a Matlab-Simulink simulator has been developed based on the toolbox SPART [16] and the Satellite Dynamic Toolbox (SDT) [15]. The toolbox SPART allows to evaluate the different terms of equation (1) and most generally the toolbox allow, for a rigid multi-body to compute the system: kinematics, differential kinematics, dynamics and forward/inverse dynamics.

An integration of the SDT into SPART allows to compute both rigid and flexible kinematics, differential kinematics, dynamics and forward/inverse dynamics.

In order to obtain numerical simulations under Matlab, each part of the robot is detailed in an Xml description. The description includes sizes, mass, inertia and the flexible mode information. Time-domain simulations are obtained with Simulink.

III. Control strategy

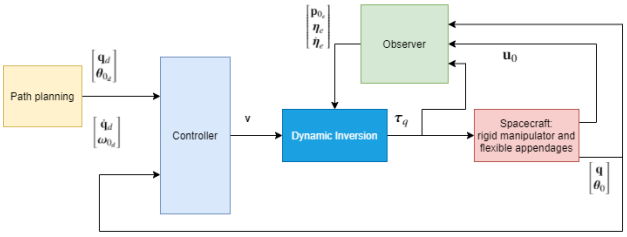

Fig. 2: Schema of the proposed control

Towards accurately controlling the manipulator under base vibration disturbances, a common attitude base and joint control is proposed. To tackle intern disturbances and improve control performances, an observer is included in the feedback linearization. In this section, a simultaneous synthesis of the control law and observer is proposed.

A. Observer structure

In order to proceed to the feedback linearization, an estimation of the vibrations (i.e. $\dot{\boldsymbol{\eta}}, \boldsymbol{\eta}$) and the linear dynamics (i.e. $\ddot{\mathbf{p}}_0$, $\dot{\mathbf{p}}_0$) is required. The observer is designed using the measure of $\dot{\mathbf{q}}$, $\boldsymbol{\omega}_0$ and the torques $\boldsymbol{\tau}_q$. A re-writing effort of (3) is required as the base angular accelerations are not provided. From the first line of (3) one can express $\dot{\omega}_0$ as:

$$\begin{aligned}\dot{\omega}_0 = &-\mathbf{H}_\omega^{-1}\begin{bmatrix}\mathbf{H}_{\omega L} & \mathbf{H}_{\omega q} & \mathbf{H}_{\omega\eta}\end{bmatrix}\begin{bmatrix}\ddot{\mathbf{p}}_0\\ \ddot{\mathbf{q}}\\ \ddot{\boldsymbol{\eta}}\end{bmatrix}\\ &-\mathbf{H}_\omega^{-1}\begin{bmatrix}\mathbf{C}_\omega & \mathbf{C}_{\omega L} & \mathbf{C}_{\omega q} & \mathbf{C}_{\omega\eta}\end{bmatrix}\begin{bmatrix}\boldsymbol{\omega}_0\\ \dot{\mathbf{p}}_0\\ \dot{\mathbf{q}}\\ \dot{\boldsymbol{\eta}}\end{bmatrix}\end{aligned} \tag{4}$$

Injecting (4) into the last three lines of (3), one can obtain the following dynamics:

$$\begin{aligned}&\mathbf{H}^*(\mathbf{q})\begin{bmatrix}\ddot{\mathbf{p}}_0\\ \ddot{\mathbf{q}}\\ \ddot{\boldsymbol{\eta}}\end{bmatrix}+\mathbf{C}^*(\mathbf{q},\dot{\mathbf{q}},\mathbf{u}_0)\begin{bmatrix}\dot{\mathbf{p}}_0\\ \dot{\mathbf{q}}\\ \dot{\boldsymbol{\eta}}\end{bmatrix}+\mathbf{K}^*(\mathbf{q})\begin{bmatrix}\mathbf{p}_0\\ \mathbf{q}\\ \boldsymbol{\eta}\end{bmatrix}\\ &+\mathbf{F}_0(\mathbf{q},\dot{\mathbf{q}},\mathbf{u}_0)\omega_0=\begin{bmatrix}0_{3\times1}\\ \boldsymbol{\tau}_q\\ 0_{n_\eta\times1}\end{bmatrix}\end{aligned} \tag{5}$$

To alleviate notation, one can pose $\mathbf{H}^{*^{-1}} = \begin{bmatrix}\mathbf{H}^1_{inv} & \mathbf{H}^2_{inv} & \mathbf{H}^3_{inv}\end{bmatrix}$ with $\mathbf{H}^1_{inv} \in \mathbb{R}^{(3+n_q+n_\eta)\times3}$, $\mathbf{H}^2_{inv} \in \mathbb{R}^{(3+n_q+n_\eta)\times n_q}$, $\mathbf{H}^3_{inv} \in \mathbb{R}^{(3+n_q+n_\eta)\times n_\eta}$. In order to estimate the vibrations and the linear dynamics of the base, one can introduce the state vector $\mathbf{x} = \begin{bmatrix}\boldsymbol{\eta}^T & \mathbf{p}_0^T & \dot{\mathbf{p}}_0^T & \dot{\mathbf{q}}^T & \dot{\boldsymbol{\eta}}^T\end{bmatrix}^T$, the command vector $\mathbf{u} = \boldsymbol{\tau}_q$ and the output vector $\mathbf{y} = \dot{\mathbf{q}}$ and with (5) one can write:

$$\begin{cases}\dot{\mathbf{x}} = \begin{bmatrix}\begin{bmatrix}\mathbf{0} & \mathbf{I}_{n\eta}\\ \mathbf{I}_3 & \mathbf{0}\end{bmatrix} & \mathbf{0} & \mathbf{0}\\ \mathbf{0} & -\mathbf{H}^{*^{-1}}\mathbf{C}^* & -\mathbf{H}^3_{inv}\mathbf{K}_\eta\end{bmatrix}\mathbf{x}\\ \quad+\begin{bmatrix}\mathbf{0}\\ \mathbf{H}^3_{inv}\end{bmatrix}\mathbf{u}+\begin{bmatrix}\mathbf{0}\\ -\mathbf{H}^{*^{-1}}\mathbf{F}_0\end{bmatrix}\omega_0\\ \quad=\mathbf{A}_e(\mathbf{q},\dot{\mathbf{q}},\mathbf{u}_0)\mathbf{x}+\mathbf{B}_e(\mathbf{q})\mathbf{u}+\mathbf{B}_0(\mathbf{q},\dot{\mathbf{q}},\mathbf{u}_0)\omega_0 \qquad (6a)\\ \mathbf{y} = \begin{bmatrix}\mathbf{0}_{n_q\times(n_\eta+3+3)} & \mathbf{I}_{n_q} & \mathbf{0}_{n_q\times n_\eta}\end{bmatrix}\mathbf{x} = \mathbf{C}_e\mathbf{x} \qquad (6b)\end{cases}$$

The state $\mathbf{x}$ is estimated as $\mathbf{x}_e$ through a linear observer of gain $\mathbf{L}$, with an LMI resolution as detailed in III-C. The observer dynamic is given by:

$$\begin{aligned}\dot{\mathbf{x}}_e = &\mathbf{A}_e(\mathbf{q},\dot{\mathbf{q}},\mathbf{u}_0)\mathbf{x}_e+\mathbf{B}_e(\mathbf{q})\mathbf{u}\\ &+\mathbf{B}_0(\mathbf{q},\dot{\mathbf{q}},\mathbf{u}_0)\omega_0+\mathbf{L}\mathbf{C}_e(\mathbf{x}-\mathbf{x}_e)\end{aligned} \tag{7}$$

The dynamic of the observation error, $\epsilon_e = \mathbf{x} - \mathbf{x}_e$, is obtained with (6) and (7) as:

$$\dot{\epsilon}_e = (\mathbf{A}_e(\mathbf{q},\dot{\mathbf{q}},\mathbf{u}_0) - \mathbf{L}\mathbf{C}_e)\epsilon_e \tag{8}$$

B. Control law structure

In the considered application, the joint and base attitude poses and dynamics, subscripted with $_d$, are provided by a path planner. Moreover, in such application, the base is actuated with slower dynamics than the manipulator, hence the necessity of decoupling all the actuators through a feedback linearization. Our proposed linearization includes the unavailable dynamics to improve the system performances.

In order to express the open-loop dynamics, a first re-writing effort of (3) is necessary to get rid of the accelerations $\ddot{\mathbf{p}}_0$, $\dot{\boldsymbol{\omega}}_r$ and $\ddot{\boldsymbol{\eta}}$. Similarly as (5) was obtained, (3) can be rewritten thusly:

$$\begin{aligned}&\mathbf{H}_{Lr\eta}\begin{bmatrix}\ddot{\mathbf{p}}_0\\ \ddot{\mathbf{q}}_r\\ \ddot{\boldsymbol{\eta}}\end{bmatrix}+\mathbf{H}_{\omega m}\begin{bmatrix}\dot{\boldsymbol{\omega}}_0\\ \ddot{\mathbf{q}}_m\end{bmatrix}\\ &+\mathbf{C}_x\mathbf{x}+\mathbf{C}_{\omega m}\begin{bmatrix}\boldsymbol{\omega}_0\\ \dot{\mathbf{q}}_m\end{bmatrix}+\mathbf{C}_r\boldsymbol{\omega}_r=\begin{bmatrix}\mathbf{0}\\ \boldsymbol{\tau}_r\\ \mathbf{0}\end{bmatrix}\end{aligned} \tag{9}$$

Finally combining (3) and (9), the open-loop model is obtained as:

$$\begin{aligned}&\mathbf{M}^*(\mathbf{q})\begin{bmatrix}\dot{\boldsymbol{\omega}}_0\\ \ddot{\mathbf{q}}_m\end{bmatrix}+\mathbf{D}^*_{\omega m}(\mathbf{q},\dot{\mathbf{q}},\mathbf{u}_0)\begin{bmatrix}\boldsymbol{\omega}_0\\ \dot{\mathbf{q}}_m\end{bmatrix}+\mathbf{D}^*_x(\mathbf{q},\dot{\mathbf{q}},\mathbf{u}_0)\mathbf{x}\\ &+\mathbf{D}^*_r(\mathbf{q},\dot{\mathbf{q}},\mathbf{u}_0)\dot{\mathbf{q}}_r=\mathbf{J}^*_\tau\begin{bmatrix}\boldsymbol{\tau}_r\\ \boldsymbol{\tau}_m\end{bmatrix}\end{aligned} \tag{10}$$

where the term $\mathbf{D}^*_x(\mathbf{q},\dot{\mathbf{q}},\mathbf{u}_0)$ expresses the impact of the vibration disturbances and the spacecraft drift on the control performances.

To simplify expressions of matrices in (10), one can introduce:

$$\mathbf{H}^{-1}_{Lr\eta} = \begin{bmatrix}\mathbf{H}_L & \mathbf{H}_{Lr} & \mathbf{H}_{L\eta}\\ \mathbf{H}^T_{Lr} & \mathbf{H}_r & \mathbf{0}\\ \mathbf{H}^T_{L\eta} & \mathbf{0} & \mathbf{H}_\eta\end{bmatrix}^{-1} = \begin{bmatrix}* & \mathbf{M}^r_{inv} & *\end{bmatrix} \tag{11}$$

where $\mathbf{M}^r_{inv} \in \mathbb{R}^{(3+n_r+n_\eta)\times n_r}$, and one can note that matrix $\mathbf{H}_{Lr\eta}$ is an inertial matrix which by definition is invertible.

From (10), feedback linearization is now easily obtained by posing (for a given desired dynamics $\mathbf{v}$) the following commanded torque $\boldsymbol{\tau}_c$:

$$\begin{aligned}\boldsymbol{\tau}_c = &\mathbf{J}^{*^+}_\tau(\mathbf{M}^*(\mathbf{q})\mathbf{v}+\mathbf{D}^*_x(\mathbf{q},\dot{\mathbf{q}},\mathbf{u}_0)\mathbf{x}_e+\mathbf{D}^*_r(\mathbf{q},\dot{\mathbf{q}},\mathbf{u}_0)\mathbf{q}_r\\ &+\mathbf{D}^*_{\omega m}(\mathbf{q},\dot{\mathbf{q}},\mathbf{u}_0)\begin{bmatrix}\boldsymbol{\omega}_0\\ \dot{\mathbf{q}}_m\end{bmatrix})\end{aligned} \tag{12}$$

where $\mathbf{J}^{*^+}_\tau$ denotes the pseudo-inverse of $\mathbf{J}^*_\tau$.

The considered torque includes the estimation of the spacecraft drift and the vibrations which, by rejecting them as well as the reaction wheels dynamics, allow to improve performances on the manipulator and spacecraft attitude control.

Introducing the tracking error, $\boldsymbol{\epsilon}_c = \left(\begin{bmatrix}\boldsymbol{\theta}_0\\ \mathbf{q}_m\end{bmatrix}_d - \begin{bmatrix}\boldsymbol{\theta}_0\\ \mathbf{q}_m\end{bmatrix}\right)$, and denote $\mathbf{v} = \begin{bmatrix}\dot{\boldsymbol{\omega}}_0\\ \ddot{\mathbf{q}}_m\end{bmatrix}_d + \mathbf{K}\begin{bmatrix}\boldsymbol{\epsilon}_c\\ \dot{\boldsymbol{\epsilon}}_c\end{bmatrix}$, by injecting (12) into (10),

the closed-loop is obtained as:

$$\begin{bmatrix}\dot{\boldsymbol{\omega}}_0\\ \ddot{\mathbf{q}}_m\end{bmatrix} = -\mathbf{M}^{*^{-1}}\mathbf{D}_x^*\boldsymbol{\epsilon}_e + \begin{bmatrix}\dot{\boldsymbol{\omega}}_0\\ \ddot{\mathbf{q}}_m\end{bmatrix}_d + \mathbf{K}\begin{bmatrix}\boldsymbol{\epsilon}_c\\ \dot{\boldsymbol{\epsilon}}_c\end{bmatrix} \tag{13}$$

The dynamic of the tracking error is then given by:

$$\ddot{\boldsymbol{\epsilon}}_c = \mathbf{M}^{*^{-1}}\mathbf{D}_x^*\boldsymbol{\epsilon}_e - \mathbf{K}\begin{bmatrix}\boldsymbol{\epsilon}_c\\ \dot{\boldsymbol{\epsilon}}_c\end{bmatrix} \tag{14}$$

Introducing the state vector $\mathbf{z} = \begin{bmatrix}\boldsymbol{\epsilon}_c^T & \dot{\boldsymbol{\epsilon}}_c^T\end{bmatrix}^T$, one can rewrite (14) as:

$$\begin{cases}\dot{\mathbf{z}} = \left(\begin{bmatrix}0 & \mathbf{I}\\ 0 & 0\end{bmatrix} + \begin{bmatrix}0\\ -\mathbf{I}\end{bmatrix}\mathbf{K}\right)\mathbf{z} + \begin{bmatrix}\mathbf{0}\\ \mathbf{M}^{*^{-1}}\mathbf{D}_x^*\end{bmatrix}\boldsymbol{\epsilon}_e & \text{(15a)}\\ \quad = (\mathbf{A}_z + \mathbf{B}_z\mathbf{K})\mathbf{z} + \mathbf{B}_\epsilon(\mathbf{q},\dot{\mathbf{q}},\mathbf{u}_0)\boldsymbol{\epsilon}_e & \\ \boldsymbol{\epsilon}_c = \begin{bmatrix}\mathbf{I} & \mathbf{0}\end{bmatrix}\mathbf{z} = \mathbf{C}_z\mathbf{z} & \text{(15b)}\end{cases}$$

As illustrated by (15), the observer and control performances are inter-dependent which is why a control and observer synthesis is simultaneously developed.

C. Simultaneous synthesis

When considering on-orbit assemblies, the manipulator motions are usually predefined. This allows to bound the state vector $\begin{bmatrix}\boldsymbol{\theta}_0^T & \mathbf{p}_0^T & \mathbf{q}_r^T & \mathbf{q}_m^T & \boldsymbol{\eta}^T\end{bmatrix}^T$ and its derivatives and consequently to bound $\mathbf{M}^*$, $\mathbf{D}_x^*$, $\mathbf{A}_e(\mathbf{q},\dot{\mathbf{q}},\mathbf{u}_0)$ and $\mathbf{B}_e(\mathbf{q})$. However, during arm maneuvers, inertia and convective matrices may significantly fluctuate. To cover such variations, it can be assumed that $\mathbf{M}^{*^{-1}}\mathbf{D}_x^*$ and $\mathbf{A}_e(\mathbf{q},\dot{\mathbf{q}},\mathbf{u}_0)$ belong to bounded sets, so that the closed-loop system both including controller and observer gains will read:

$$\begin{cases}\dot{\mathbf{z}} = (\mathbf{A}_z + \mathbf{B}_z\mathbf{K})\mathbf{z} + (\mathbf{B}_\epsilon + \Delta\mathbf{B}_\epsilon)\boldsymbol{\epsilon}_e & \text{(16a)}\\ \dot{\boldsymbol{\epsilon}}_e = ((\mathbf{A}_e + \Delta\mathbf{A}_e) - \mathbf{L}\mathbf{C}_e)\boldsymbol{\epsilon}_e & \text{(16b)}\end{cases}$$

where $\Delta\mathbf{B}_\epsilon$ and $\Delta\mathbf{A}_e$ respectively correspond to the variation of $\mathbf{B}_\epsilon$ and $\mathbf{A}_e$ during the considered maneuver.

Using the extended state vector $\mathbf{X} = \begin{bmatrix}\mathbf{z}^T & \boldsymbol{\epsilon}_e^T\end{bmatrix}^T$ a compact version is obtained:

$$\begin{cases}\dot{\mathbf{X}} = \begin{bmatrix}\mathbf{A}_z + \mathbf{B}_z\mathbf{K} & \mathbf{B}_\epsilon + \Delta\mathbf{B}_\epsilon\\ \mathbf{0} & \mathbf{A}_e + \Delta\mathbf{A}_e - \mathbf{L}\mathbf{C}_e\end{bmatrix}\mathbf{X} & \text{(17a)}\\ \boldsymbol{\epsilon}_c = \begin{bmatrix}\mathbf{C}_z & \mathbf{0}\end{bmatrix}\mathbf{X} & \text{(17b)}\end{cases}$$

We assume that the estimation error verifies $\boldsymbol{\epsilon}_{e_0}^T\mathbf{E}\boldsymbol{\epsilon}_{e_0} \leq 1$ for a given positive definite matrix E, where $\boldsymbol{\epsilon}_{e_0}$ is the initial condition of the observer error. Based on the following proposition, the observer and controller gain are obtained with a LMI resolution to ensure both stability and performance properties.

1) Proposition: If there exist symmetric positive definite matrices $\mathbf{Q}_z$, $\mathbf{P}_\epsilon$ and matrices $\mathbf{W}_z$, $\mathbf{W}_\epsilon$ such that for a given scalar $\gamma > 0$:

$$\begin{bmatrix}(\mathbf{A}_z\mathbf{Q}_z + \mathbf{B}_z\mathbf{W}_z)^{\mathbf{s}} & (\mathbf{B}_\epsilon + \Delta\mathbf{B}_\epsilon) & \\ * & (\mathbf{P}_\epsilon(\mathbf{A}_e + \Delta\mathbf{A}_e))^{\mathbf{s}} & \\ * & * & \\ & & \mathbf{Q}_z\mathbf{C}_z^T\\ & -(\mathbf{W}_\epsilon\mathbf{C}_e)^{\mathbf{s}} & \mathbf{0}\\ & & -\gamma^2\mathbf{I}\end{bmatrix} < 0 \tag{18a}$$

$$\mathbf{P}_\epsilon < \mathbf{E} \tag{18b}$$

where $\mathbf{X}^{\mathbf{s}} = \mathbf{X} + \mathbf{X}^T$, then the system is stable and the outputs verify:

$$\int_0^\infty \boldsymbol{\epsilon}_c^T\boldsymbol{\epsilon}_c dt < \gamma^2 \tag{19}$$

for any conditions $\mathbf{z}(0) = 0$ and $\boldsymbol{\epsilon}_{e_0} \in \{\epsilon \mid \epsilon^T\mathbf{E}\epsilon \leq 1\}$. Moreover, the gains are obtained as:

$$\begin{cases}\mathbf{K} = \mathbf{W}_z\mathbf{Q}_z^{-1} & \text{(20a)}\\ \mathbf{L} = \mathbf{P}_\epsilon^{-1}\mathbf{W}_e & \text{(20b)}\end{cases}$$

2) Proof: Let us introduce the Lyapunov function:

$$\mathbf{V}(\mathbf{X}) = \mathbf{z}^T\mathbf{P}_z\mathbf{z} + \boldsymbol{\epsilon}_e^T\mathbf{P}_\epsilon\boldsymbol{\epsilon}_e \tag{21}$$

such that $\dot{\mathbf{V}} + \gamma^{-2}\boldsymbol{\epsilon}_c^T\boldsymbol{\epsilon}_c < 0$ for a given $\gamma > 0$.

By integration:

$$\begin{aligned}\int_0^{T_f}(\dot{\mathbf{V}} + \boldsymbol{\epsilon}_c^T\boldsymbol{\epsilon}_c)dt < 0 \Rightarrow \int_0^{T_f}\boldsymbol{\epsilon}_c^T\boldsymbol{\epsilon}_c dt < \gamma^2(\mathbf{V}_0 - \mathbf{V}_{T_f})\\ \Rightarrow \int_0^\infty \boldsymbol{\epsilon}_c^T\boldsymbol{\epsilon}_c dt < \gamma^2\mathbf{V}_0\end{aligned} \tag{22}$$

with $\mathbf{V}_0 = \mathbf{z}_0^T\mathbf{P}_z\mathbf{z}_0 + \boldsymbol{\epsilon}_{e_0}^T\mathbf{P}_\epsilon\boldsymbol{\epsilon}_{e_0}$. For $\mathbf{z}_0 = 0_{2\times(3+n_m)}$, $\mathbf{V}_0 = \boldsymbol{\epsilon}_{e_0}^T\mathbf{P}_\epsilon\boldsymbol{\epsilon}_{e_0}$ and if $\boldsymbol{\epsilon}_{e_0}^T\mathbf{P}_\epsilon\boldsymbol{\epsilon}_{e_0} \leq \boldsymbol{\epsilon}_{e_0}^T\mathbf{E}\boldsymbol{\epsilon}_{e_0} \leq 1$ then (19) is verified. This condition is enforced by $\mathbf{P}_\epsilon \leq \mathbf{E}$.

The condition $\dot{\mathbf{V}} + \gamma^{-2}\boldsymbol{\epsilon}_c^T\boldsymbol{\epsilon}_c < 0$ is equivalent to:

$$\begin{bmatrix}(\mathbf{P}_z(\mathbf{A}_z + \mathbf{B}_z\mathbf{K}))^{\mathbf{s}} + \gamma^{-2}\mathbf{C}_z^T\mathbf{C}_z & \\ * & \\ & \mathbf{P}_z(\mathbf{B}_\epsilon + \Delta\mathbf{B}_\epsilon)\\ & (\mathbf{P}_\epsilon(\mathbf{A}_e + \Delta\mathbf{A}_e - \mathbf{L}\mathbf{C}_e))^{\mathbf{s}}\end{bmatrix} < 0 \tag{23}$$

The Schur complement is given by:

$$\begin{bmatrix}(\mathbf{P}_z(\mathbf{A}_z + \mathbf{B}_z\mathbf{K}))^{\mathbf{s}} & \mathbf{P}_z(\mathbf{B}_\epsilon + \Delta\mathbf{B}_\epsilon) & \\ * & (\mathbf{P}_\epsilon(\mathbf{A}_e + \Delta\mathbf{A}_e - \mathbf{L}\mathbf{C}_e))^{\mathbf{s}} & \\ * & * & \\ & & \mathbf{C}_z^T\\ & & \mathbf{0}\\ & & -\gamma^2\mathbf{I}\end{bmatrix} < 0 \tag{24}$$

Pre and post multiplying the above matrix matrix by $\text{diag}(\mathbf{Q}_z,\mathbf{I},\mathbf{I}) = \text{diag}(\mathbf{P}_z^{-1},\mathbf{I},\mathbf{I})$ and introducing the variable changes $\mathbf{W}_e = \mathbf{P}_\epsilon\mathbf{L}$ and $\mathbf{W}_z = \mathbf{K}\mathbf{Q}_z$ one obtains (18a) which concludes the proof.

In order to resolve (18a), one can introduce the positive constants ρ_1 and ρ_2 such that $\|\Delta\mathbf{A}_e\| \leq \rho_1$ and $\|\Delta\mathbf{B}_\epsilon\| \leq \rho_2$ and respectively replace in (18a) $\Delta\mathbf{A}_e$ and $\Delta\mathbf{B}_\epsilon$ by $\rho_1\mathbf{I}$ and $\rho_2\mathbf{I}$.

IV. Illustration of the proposed method

In order to illustrate our proposed method, the on-orbit deployment of the PULSAR telescope [3], represented in Fig. 1, is considered. The deployment is divided in different motions, in which either the manipulator moves a mirror tile or a bundle of tiles or is reaching to grab a tile.

The PULSAR spacecraft is equipped with an 8 DOF manipulator with a mass of 327 kg and an augmented version of the CAESAR's manipulator [17]. According to

the considered moment of the scenario, the manipulator end-effector may handle a mirror tile weighting 44K kg. The base attitude is actuated with 6 identical reaction wheels with an angular momentum at nominal speed of 12 Nms. Between the solar array and the beams of the solar shields, 22 flexible modes are considered. Through the complete deployment scenario, the inertia of the system is varying between $\mathbf{I}_{xx} \in \begin{bmatrix}41077 & 45324\end{bmatrix} kg.m^2$, $\mathbf{I}_{yy} \in \begin{bmatrix}132030 & 203470\end{bmatrix} kg.m^2$, $\mathbf{I}_{zz} \in \begin{bmatrix}116870 & 192530\end{bmatrix} kg.m^2$ for a total mass of 6892 kg.

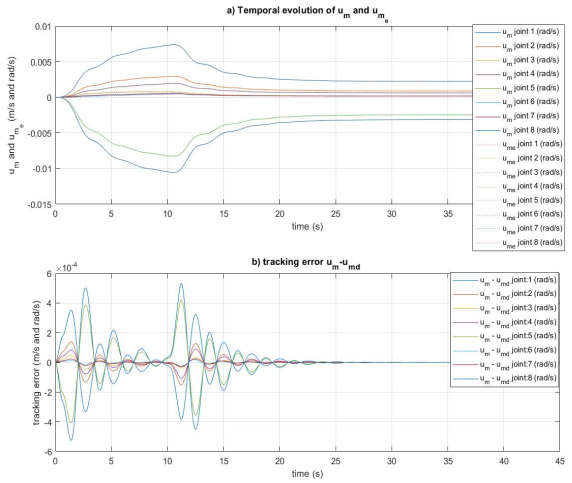

Fig. 3: a) Evolution of $\dot{\mathbf{u}}_m$ and $\dot{\mathbf{u}}_{m_e}$;b) Evolution of $\boldsymbol{\epsilon}_c$

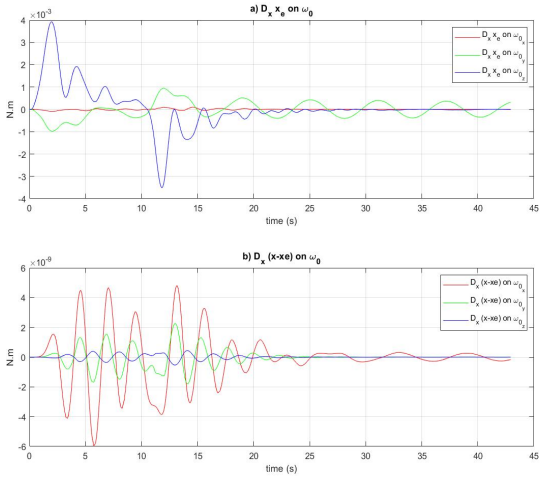

Fig. 4: a)Terms of $\mathbf{D}_x^* \mathbf{x}_e$ impacting on $\boldsymbol{\omega}_0$; b)Terms of $\mathbf{D}_x^*(\mathbf{x} - \mathbf{x}_e)$ impacting on $\boldsymbol{\omega}_0$

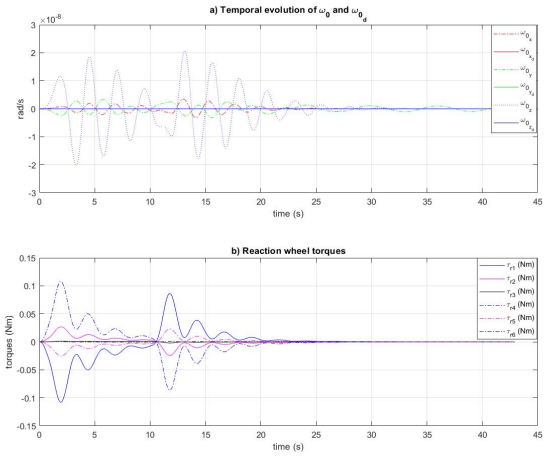

Fig. 5: a) Evolution of $\boldsymbol{\omega}_0$ and $\boldsymbol{\omega}_{0_d}$;b) Evolution of $\boldsymbol{\tau}_r$

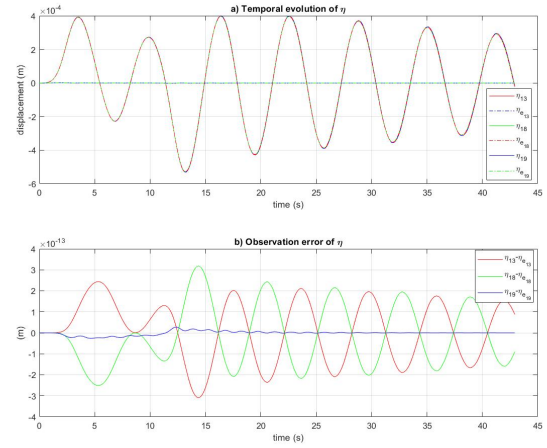

Fig. 6: Evolution of the three most impacting modes, a) Evolution of $\boldsymbol{\eta}$ and $\boldsymbol{\eta}_e$;b) Evolution of the observer error of the three most impacting flexible modes

The YALMIP toolbox [18] with the mosek solver is used to solve the large dimension LMI in III-C.1 while minimising the parameter λ.

As illustrated in Fig. 3, in which the manipulator joint velocities and the evolution of the associated tracking error $\dot{\boldsymbol{\epsilon}}_c$ are plotted, the joint manipulator are precisely controlled however the disturbances acting on the spacecraft base. Likewise the proposed control allows to keep the base attitude velocity at its initial rate of zeros rad/s as illustrated in Fig. 5 where the evolution of Euler angles and ω_0 are plotted. Moreover the torques $\boldsymbol{\tau}_r$ are successfully maintain under there saturated value of $0.12Nm$ [3]. The observer performances are illustrated in Fig. 6 with the estimation of the flexible modes impacting the most the spacecraft base. Finally the proposed method interest is illustrated by Fig. 4, in which the impacts of $\mathbf{D}_x^* \mathbf{x}_e$ on ω_0 control are highlighted. Adding the estimation have allowed to reduced the disturbance effects on the torques.

V. Conclusion

In this paper, the general tools for a common control of the base and manipulator actuators are developed to achieve high-precision manipulator control for on-orbit assembly scenarios in presence of vibration disturbances and system variations. The common control, motivated by our previous work on system analysis [13], allows to improve the control performances with a better use of actuators. By detailing the rigid-flexible dynamics of the spacecraft, the disturbances are tackled in the feedback linearization with a better efficiency than with a classical unknown disturbance observer. The proposed method has shown feasibility on a real on-orbit deployment scenario and future works are expected to consider larger system variations to be applied during the complete deployment.

VI. Appendix

A. Detail of equation (5)

$$\mathbf{H}^* = \begin{bmatrix} -\mathbf{H}_{L\omega}\mathbf{H}_\omega^{-1}\mathbf{H}_{\omega L} + \mathbf{H}_L & -\mathbf{H}_{L\omega}\mathbf{H}_\omega^{-1}\mathbf{H}_{\omega m} + \mathbf{H}_{Lq} \\ -\mathbf{H}_{\omega q}^T\mathbf{H}_\omega^{-1}\mathbf{H}_{\omega L} + \mathbf{H}_{Lq}^T & -\mathbf{H}_{\omega q}^T\mathbf{H}_\omega^{-1}\mathbf{H}_{\omega q} + \mathbf{H}_q \\ -\mathbf{H}_{\omega\eta}^T\mathbf{H}_\omega^{-1}\mathbf{H}_{\omega L} + \mathbf{H}_{L\eta}^T & -\mathbf{H}_{\omega\eta}^T\mathbf{H}_\omega^{-1}\mathbf{H}_{\omega q} \\ & \end{bmatrix}$$
$$\begin{bmatrix} -\mathbf{H}_{L\omega}\mathbf{H}_\omega^{-1}\mathbf{H}_{\omega\eta} + \mathbf{H}_{L\eta} \\ -\mathbf{H}_{\omega q}^T\mathbf{H}_\omega^{-1}\mathbf{H}_{\omega\eta} \\ -\mathbf{H}_{\omega\eta}^T\mathbf{H}_\omega^{-1}\mathbf{H}_{\omega\eta} + \mathbf{H}_\eta \end{bmatrix}$$

$$\mathbf{C}^* = \begin{bmatrix} -\mathbf{H}_{L\omega}\mathbf{H}_\omega^{-1}\mathbf{C}_{\omega L} + \mathbf{C}_L & -\mathbf{H}_{L\omega}\mathbf{H}_\omega^{-1}\mathbf{C}_{\omega q} + \mathbf{C}_{Lq} \\ -\mathbf{H}_{\omega q}^T\mathbf{H}_\omega^{-1}\mathbf{C}_{\omega L} + \mathbf{C}_{Lq}^T & -\mathbf{H}_{\omega q}^T\mathbf{H}_\omega^{-1}\mathbf{C}_{\omega q} + \mathbf{C}_q \\ -\mathbf{H}_{\omega\eta}^T\mathbf{H}_\omega^{-1}\mathbf{C}_{\omega L} + \mathbf{C}_{L\eta}^T & -\mathbf{H}_{\omega\eta}^T\mathbf{H}_\omega^{-1}\mathbf{C}_{\omega q} \\ & \end{bmatrix}$$
$$\begin{bmatrix} -\mathbf{H}_{L\omega}\mathbf{H}_\omega^{-1}\mathbf{C}_{\omega\eta} + \mathbf{C}_{L\eta} \\ -\mathbf{H}_{\omega q}^T\mathbf{H}_\omega^{-1}\mathbf{C}_{\omega\eta} \\ -\mathbf{H}_{\omega\eta}^T\mathbf{H}_\omega^{-1}\mathbf{C}_{\omega\eta} + \mathbf{C}_\eta \end{bmatrix}$$

$$\mathbf{K}^* = \begin{bmatrix} \mathbf{0}_{(3+n_q)} & \mathbf{0}_{(3+n_q)\times n_\eta} \\ \mathbf{0}_{n_\eta\times(3+n_q)} & \mathbf{K}_\eta \end{bmatrix}$$

$$\mathbf{F}_0 = \begin{bmatrix} -\mathbf{H}_{\omega q}^T\mathbf{H}_\omega^{-1}\mathbf{C}_\omega + \mathbf{C}_{L\omega} \\ -\mathbf{H}_{\omega q}^T\mathbf{H}_\omega^{-1}\mathbf{C}_\omega + \mathbf{C}_{\omega q}^T \\ -\mathbf{H}_{\omega\eta}^T\mathbf{H}_\omega^{-1}\mathbf{C}_\omega + \mathbf{C}_{\omega\eta}^T \end{bmatrix}$$

B. Detail of equation (10)

One can pose $\mathbf{H}_{Lr\eta}^\diamond = \begin{bmatrix} \mathbf{H}_{\omega L} & \mathbf{H}_{\omega r} & \mathbf{H}_{\omega\eta} \\ \mathbf{H}_{Lm}^T & \mathbf{0} & \mathbf{0} \end{bmatrix} \mathbf{H}_{Lr\eta}^{-1}$, then:

$$\mathbf{M}^* = \begin{bmatrix} \mathbf{H}_\omega & \mathbf{H}_{\omega m} \\ \mathbf{H}_{\omega m}^T & \mathbf{H}_m \end{bmatrix} - \mathbf{H}_{Lr\eta}^\diamond \begin{bmatrix} \mathbf{H}_{L\omega} & \mathbf{H}_{Lm} \\ \mathbf{H}_{\omega r}^T & \mathbf{0} \\ \mathbf{H}_{\omega\eta}^T & \mathbf{0} \end{bmatrix}$$

$$\mathbf{D}_{\omega m}^* = \begin{bmatrix} \mathbf{C}_\omega & \mathbf{C}_{\omega m} \\ \mathbf{C}_{\omega m}^T & \mathbf{C}_m \end{bmatrix} - \mathbf{H}_{Lr\eta}^\diamond \begin{bmatrix} \mathbf{C}_{L\omega} & \mathbf{C}_{Lm} \\ \mathbf{C}_{\omega r}^T & \mathbf{0} \\ \mathbf{C}_{\omega\eta}^T & \mathbf{0} \end{bmatrix}$$

$$\mathbf{D}_x^* = \begin{bmatrix} \mathbf{C}_{\omega L} & \mathbf{0} & \mathbf{0} & \mathbf{C}_{\omega\eta} & \mathbf{0} & \mathbf{0} \\ \mathbf{C}_{Lm}^T & \mathbf{0} & \mathbf{0} & \mathbf{0} & \mathbf{0} & \mathbf{0} \end{bmatrix}$$
$$- \mathbf{H}_{Lr\eta}^\diamond \begin{bmatrix} \mathbf{C}_L & \mathbf{0} & \mathbf{0} & \mathbf{C}_{L\eta} & \mathbf{0} & \mathbf{0} \\ \mathbf{C}_{Lr}^T & \mathbf{0} & \mathbf{0} & \mathbf{0} & \mathbf{0} & \mathbf{0} \\ \mathbf{C}_{L\eta}^T & \mathbf{0} & \mathbf{0} & \mathbf{C}_\eta & \mathbf{K}_\eta & \mathbf{0} \end{bmatrix}$$

$$\mathbf{D}_r^* = \begin{bmatrix} \mathbf{C}_{\omega r} \\ \mathbf{0} \end{bmatrix} - \mathbf{H}_{Lr\eta}^\diamond \begin{bmatrix} \mathbf{C}_{Lr} \\ \mathbf{C}_r \\ \mathbf{0} \end{bmatrix}$$

$$\mathbf{J}_\tau^* = \begin{bmatrix} -\begin{bmatrix} \mathbf{H}_{\omega L} & \mathbf{H}_{\omega r} & \mathbf{H}_{\omega\eta} \end{bmatrix} \mathbf{M}_{inv}^r & \mathbf{0} \\ -\begin{bmatrix} \mathbf{H}_{Lm}^T & \mathbf{0} & \mathbf{0} \end{bmatrix} \mathbf{M}_{inv}^r & \mathbf{I} \end{bmatrix}$$

VII. Acknowledgement

The PULSAR project is funded under the European Commission's Horizon 2020 Space Strategic Research Cluster Operational Grants, grant number 821858. The authors would like to thank M. Aurélien Cuffolo, from Thales AleniaSpace in France, partner in the PULSAR consortium, for providing inputs on mission analysis, spacecraft sizing and AOCS models.

References

[1] Flores-Abad *et al.*, "A review of space robotics technologies for on-orbit servicing," *Progress in Aerospace Sciences*, vol. 68, pp. 1–26, 2014.

[2] W.-J. Li *et al.*, "On-orbit service (oos) of spacecraft: A review of engineering developments," *Progress in Aerospace Sciences*, vol. 108, pp. 32–120, 2019.

[3] M. Rognant *et al.*, "Autonomous assembly of large structures in space: a technology review," in *8th European Conference for Aeronautics and Aerospace Sciences (EUCASS)*, 2019.

[4] P. Zarafshan *et al.*, "Adaptive hybrid suppression control of space free-flying robots with flexible appendages." *Robotica*, vol. 34, no. 7, pp. 1464–1485, 2016.

[5] W. Hu *et al.*, "Semi-active vibration control of two flexible plates using an innovative joint mechanism," *Mechanical Systems and Signal Processing*, vol. 130, pp. 565–584, 2019.

[6] J. Qiao *et al.*, "High-precision attitude tracking control of space manipulator system under multiple disturbances," *IEEE Transactions on Systems, Man, and Cybernetics: Systems*, 2019.

[7] A. M. Giordano *et al.*, "Workspace fixation for free-floating space robot operations," in *2018 IEEE International Conference on Robotics and Automation (ICRA)*. IEEE, 2018, pp. 889–896.

[8] A. M. Giordano, C. Ott, and A. Albu-Schäffer, "Coordinated control of spacecraft's attitude and end-effector for space robots," *IEEE Robotics and Automation Letters*, vol. 4, no. 2, pp. 2108–2115, 2019.

[9] A. Pisculli and P. Gasbarri, "A minimum state multibody/fem approach for modeling flexible orbiting space systems," *Acta Astronautica*, vol. 110, pp. 324–340, 2015.

[10] D. Meng *et al.*, "Vibration suppression control of free-floating space robots with flexible appendages for autonomous target capturing," *Acta Astronautica*, vol. 151, pp. 904–918, 2018.

[11] K. Li, Q. Tian, J. Shi, and D. Liu, "Assembly dynamics of a large space modular satellite antenna," *Mechanism and Machine Theory*, vol. 142, p. 103601, 2019.

[12] M. Wilde *et al.*, "Equations of motion of free-floating spacecraft-manipulator systems: An engineer's tutorial," *Frontiers in Robotics and AI*, vol. 5, p. 41, 2018.

[13] M. Rognant *et al.*, "Kinematic indices of rotation-floating space robots for on-orbit servicing," in *IFToMM World Congress on Mechanism and Machine Science*. Springer, 2019, pp. 3107–3116.

[14] Y. Wu *et al.*, "Attitude control for on-orbit servicing spacecraft using hybrid actuator," *Advances in Space Research*, vol. 61, no. 6, 2018.

[15] D. Alazard, C. Cumer, and K. Tantawi, "Linear dynamic modeling of spacecraft with various flexible appendages and on-board angular momentums," 2008.

[16] J. Virgili-Llop *et al.*, "SPART: an open-source modeling and control toolkit for mobile-base robotic multibody systems with kinematic tree topologies," https://github.com/NPS-SRL/SPART.

[17] A. Beyer *et al.*, "Caesar: Space robotics technology for assembly, maintenance, and repair," in *Proceedings of the International Astronautical Congress, IAC*, 2018.

[18] J. Löfberg, "Yalmip : A toolbox for modeling and optimization in matlab," in *In Proceedings of the CACSD Conference*, Taipei, Taiwan, 2004.